Engineering Science
2026, Vol. 11, No. 3, pp. 59–68
https://doi.org/10.11648/j.es.20261103.11

SciencePG
Science Publishing Group

Research Article

Effects of Shearing Rate on the Stress-strain Response and Shear Strength of Red Clay: A Case Study of Wolaita Sodo City, Ethiopia

Wopnesh Bassa Beyene, Eyob Shanka Koyra*, Jemal Aliy Gobena

Department of Civil Engineering, Wolaita Sodo University, Wolaita Sodo, Ethiopia

Abstract

Rapid infrastructure development in Wolaita Sodo City, Ethiopia, relies extensively on locally available tropical red clay, whose high plasticity and compressibility result in complex mechanical behavior. However, the sensitivity of this residual soil to shearing rate under rapid and transient loading conditions remains poorly understood. This study investigates the effects of shearing rate on the stress-strain response, peak deviator stress, and shear strength of Wolaita Sodo red clay. Disturbed and undisturbed samples were collected from eight test pits distributed across four sub-cities at depths of 2.5-3.0 m. The experimental program included index-property characterization, Modified Proctor compaction, and Unconsolidated Undrained (UU) and Consolidated Undrained (CU) triaxial compression tests conducted at axial displacement rates of 0.01, 0.1, and 1.0 mm/min. The results demonstrate pronounced rate-dependent behavior. Increasing the displacement rate from 0.01 to 1.0 mm/min increased the peak deviator stress and undrained shear strength, while reducing the axial strain at failure, indicating a transition from more ductile to more brittle deformation. The CU tests also showed increases in the derived effective strength parameters, (c') and ϕ', with increasing shearing rate, although the magnitude of this response varied among test pits and confining pressures. Higher confining pressures generally increased the overall shear resistance. These findings provide site-specific experimental parameters for evaluating foundations, slopes, and other geotechnical structures constructed on tropical red clay deposits.

Keywords

Shearing-rate Sensitivity, Tropical Residual Clay, Triaxial Compression, Undrained Shear Strength, Peak Deviator Stress, Stress-strain Behavior

1. Introduction

In geotechnical engineering, understanding the rate-dependent behavior of cohesive soils is essential for evaluating the stability and deformation response of civil infrastructure under dynamic and transient loading conditions. The strain rate, defined as the rate of mechanical deformation, can significantly influence the stress-strain response, pore-water-pressure development, and shear strength of clayey soils [1, 2]. In practice, subsoils are subjected to a wide range of loading rates, from slow, quasi-static consolidation during embankment construction to rapid shearing associated with traffic loading, slope failures, pile driving, and seismic events. Ne-

*Correspondence: Eyob Shanka Koyra (eyobshanka8@gmail.com)

Received: 12 October 2026; **Accepted:** 26 October 2026; **Published:** 9 November 2026

Copyright: © The Author(s), 2026. Published by Science Publishing Group. This is an **Open Access** article, distributed under the terms of the Creative Commons Attribution 4.0 License (http://creativecommons.org/licenses/by/4.0/), which permits unrestricted use, distribution and reproduction in any medium, provided the original work is properly cited.

glecting rate-dependent behavior may lead to inaccurate estimates of bearing capacity, slope stability, and foundation settlement, thereby compromising the safety and serviceability of geotechnical structures [3, 4].

Cohesive soils, particularly fine-grained residual clays with high plasticity and compressibility, exhibit complex and nonlinear mechanical responses that depend strongly on loading rate. Changes in shearing rate can affect clay-particle reorientation, viscous resistance, and drainage conditions during deformation [5, 6] Under undrained conditions, high strain rates may restrict pore-water-pressure dissipation, modify effective-stress paths, and produce an apparent increase in shear strength because of viscous resistance. In contrast, low strain rates provide more time for pore-pressure redistribution and creep deformation, which may contribute to progressive failure. Therefore, quantifying the rate dependence of stress-strain behavior and shear strength parameters, including effective cohesion ((c')) and effective friction angle (ϕ'), is important for reliable constitutive modeling and geotechnical design in cohesive soil deposits [7, 8].

Tropical red clays are widely distributed across the Main Ethiopian Rift and the East African Plateau and commonly serve as foundation soils and construction materials in rapidly developing urban centers such as Wolaita Sodo City, Ethiopia. These soils are derived predominantly from the intense weathering of volcanic parent rocks and may exhibit distinctive mineralogical compositions, high fines contents, and structured particle arrangements that contribute to complex geomechanical behavior [9, 10]. Despite rapid infrastructure development in Wolaita Sodo City, including buildings, highway embankments, and excavations, geotechnical design commonly relies on conventional soil parameters obtained at a single standard laboratory loading rate. Consequently, limited information is available on the effects of loading rate on the stress-strain response, failure characteristics, and shear strength of Wolaita Sodo red clay.

This study presents an experimental investigation of the rate-dependent behavior of Wolaita Sodo red clay. Disturbed and undisturbed soil samples were collected from eight representative test pits distributed across four sub-cities at depths of 2.5-3.0 m. The experimental program included index-property characterization comprising particle-size distribution, Atterberg limits, specific gravity, natural moisture content, and compaction characteristics, followed by Unconsolidated Undrained (UU) and Consolidated Undrained (CU) triaxial compression tests at three axial displacement rates: 0.01, 0.1, and 1.0 mm/min. The study evaluates the effects of loading rate and confining pressure on peak deviator stress, undrained shear strength, axial strain at failure, and effective shear strength parameters. The results provide site-specific evidence of the rate-dependent behavior of tropical residual red clay and establish useful parameters for the design and assessment of infrastructure founded on similar soils.

2. Materials and Methods

2.1. Study Area and Geotechnical Sampling

The study was conducted in Wolaita Sodo City, the administrative center of Wolaita Zone in southern Ethiopia, at approximately 6 °54' N and 37 °45' E. The city is situated at elevations ranging from approximately 1,600 to 2,100 m above mean sea level and has a subtropical highland climate characterized by distinct wet and dry seasons [11-14] The regional geology is dominated by highly weathered volcanic rocks, which have formed thick deposits of tropical residual red clay. The locations and elevations of the test pits are summarized in Table 1, and the study-area map is presented in Figure 1.

Table 1. *Locations and field information for the test pits.*

Test pits	Sample depth, m	Location description	Latitude (DMS)	Longitude (DMS)	Elevation (m)	Sub-city
TP1	3	Around city municipality	6°51'57.954" N	37°45'45.990" E	2072	Arada
TP2	2.5	Rufael church	6°52'48.52" N	37°45'26.423" E	2110	Arada
TP3	3	Around Isreal church	6°52'32.33" N	37°46'54.066" E	2165	Markato
TP4	2.5	Mebrat Hail kalhiwot church	6°50'55.326" N	37°46'12.041" E	2033	Markato
TP5	2.5	Sodo Agricultural college	6°50'25.896" N	37°45'29.754" E	1930	Fana
TP6	2.5	Kera Meseret kirstos church	6°50'56.423" N	37°45'58.608" E	1970	Fana
TP7	3	Dombosco primary school	6°51'40.745" N	37°44'52.607" E	1951	Mehal
TP8	2.5	Konto full Gospel church	6°50'46.199" N	37°45'12.005" E	1952	Mehal

DMC = Indicates Degree Minute Second.

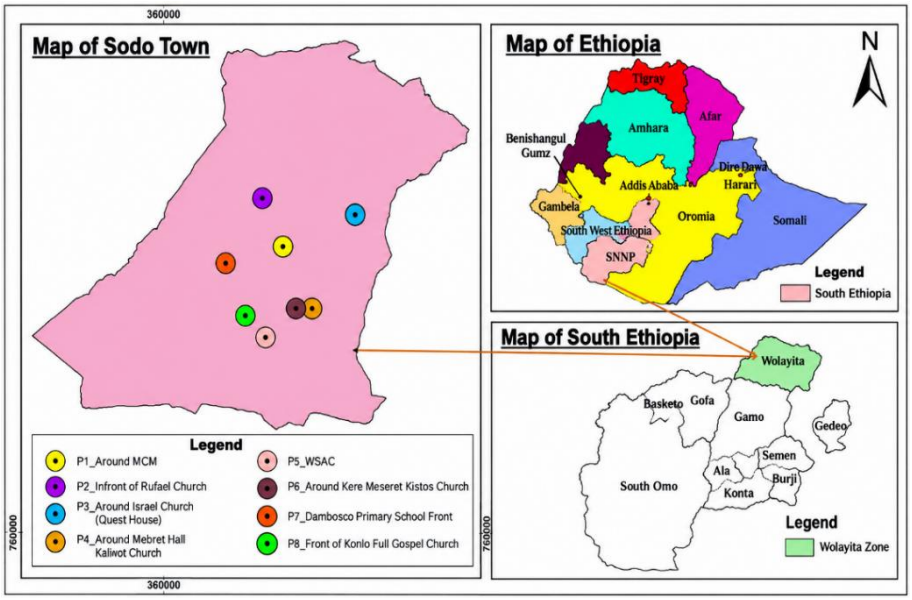


Figure 1. *Location map of the study area.*

To account for the spatial variability of the soil within the urban expansion area, purposive sampling was conducted across four Sub cities of Wolaita Sodo City. Eight representative test pits, designated TP1-TP8, were excavated to depths of 2.5-3.0 m. These depths were selected to represent the zone of influence of typical shallow foundations and road subgrades in the study area. The sampling locations and corresponding field information are presented in Table 1.

Both disturbed and undisturbed samples were collected from the test pits. Undisturbed samples were carefully extracted to preserve their natural structure, sealed to minimize moisture loss, and transported to the Geotechnical Engineering Laboratory of Wolaita Sodo University. Disturbed bulk samples were collected in sealed containers and subsequently air-dried at room temperature, gently disaggregated without crushing individual particles, and prepared for index-property and compaction tests. The undisturbed samples were retained in their natural condition for triaxial testing.

2.2. Laboratory Testing Standards

The physical index, compaction, and shear-strength properties of the red clay were determined using standard ASTM and AASHTO procedures. The laboratory testing program and the corresponding standards are summarized in Table 2.

Table 2. *Laboratory testing program and applicable standards.*

No.	Test or Parameter	Governing standard	Main output
1	Natural moisture content	ASTM D2216	In-situ moisture state via oven drying method
2	Specific gravity	ASTM D854	Particle density using a calibrated water pycnometer
3	Particle size distribution	ASTM D422	Wet sieve and hydrometer analysis
4	Atterberg limits	ASTM D4318	Liquid limit, plastic limit and plasticity index
5	Soil classification	ASTM D2487/AASHTO M145	USCS (plasticity chart) and AASHTO (Group index
6	Modified Compaction	ASTM D1557	Maximum dry density and Optimum moisture content
7	Unconsolidated undrained (UU) triaxial test	ASTM D2850	Total stress undrained shear strength at varying strain rates
8	Unconsolidated Drained (CU) triaxial test	ASTM D4767	Effective shear strength parameters (c' and ϕ')

3. Results and Discussion

3.1. Physical Index Characterization and Soil Classification

The physical index properties of the red clay collected from eight test pits (TP1-TP8) are summarized in Table 3. The natural moisture content ranged from 32.46% at TP3 to 39.08% at TP2, with a mean value of 36.47%. These relatively high moisture contents indicate the substantial water-retention capacity of the tropical residual clay and may contribute to increased compressibility and reduced shear resistance under saturated conditions [15, 16]. The specific gravity varied from 2.59 at TP2 to 2.75 at TP7, with an average of 2.65. The relatively high values measured at TP7 and TP8 may be associated with local variations in mineralogical composition, including the presence of iron- and aluminium-rich weathering products commonly found in tropical residual soils [17].

The particle-size analyses showed that 77.20-88.97% of the soil passed the No. 200 sieve (0.075mm), confirming the predominance of fine-grained particles. The Liquid Limit (LL) ranged from 42.16% to 49.47%, with a mean of 45.31%, whereas the Plastic Limit (PL) varied from 24.49% to 27.72%, with a mean of 25.87%. The Plasticity Index (PI) ranged from 17.07% to 22.45%, with an average of 19.44% [18]. These results indicate a soil with intermediate plasticity and a relatively high affinity for water.

All samples plotted above the A-line on the Casagrande plasticity chart and within the intermediate-plasticity clay region. Accordingly, the soils were classified as CI, or inorganic clay of intermediate plasticity, according to the USCS. Under the AASHTO system, all samples were classified as A-7-6, with Group Index values ranging from 15 to 22. This classification indicates a fine-grained soil with limited drainage, moderate-to-high compressibility, and potential for strength reduction and work-softening when subjected to increased moisture or undrained loading [19]. The grain-size distribution curves, plasticity chart, and liquid-limit curves are presented in Figures 2-4, respectively.

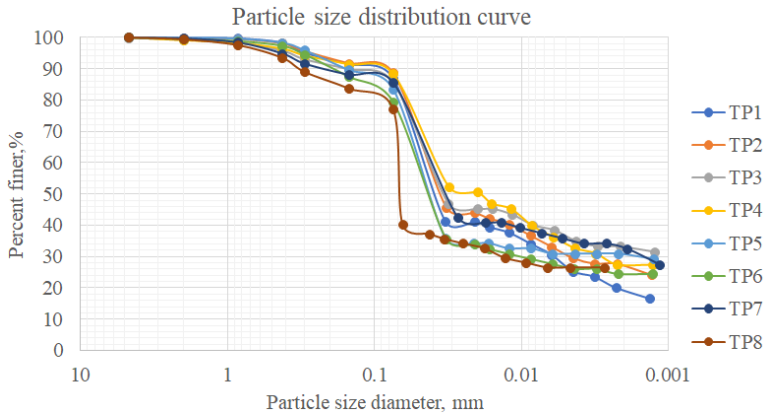


Figure 2. *Grain size distribution curves.*

Table 3. *Physical index properties and classification of Wolaita Sodo red clay.*

Test pit	Fines passing #200 (%)	Liquid limit (%)	Plastic limit (%)	Plasticity index (%)	AASHTO code	USCS code	Specific gravity	Natural moisture content (%)	Soil color
TP1	88.97	48.05	27.72	20.33	A-7-6 (21)	CI	2.60	38.89	Red
TP2	88.75	49.47	27.02	22.45	A-7-6 (22)	CI	2.59	39.08	Red
TP3	85.73	42.16	25.09	17.07	A-7-6 (16)	CI	2.65	32.46	Red
TP4	88.44	44.47	25.79	18.68	A-7-6 (18)	CI	2.62	33.03	Red
TP5	83.59	45.43	26.31	19.12	A-7-6 (17)	CI	2.62	37.34	Red
TP6	79.49	43.38	25.05	18.33	A-7-6 (15)	CI	2.65	36.17	Red
TP7	85.65	44.16	24.49	19.67	A-7-6 (18)	CI	2.75	37.64	Red
TP8	77.20	45.35	25.51	19.84	A-7-6 (16)	CI	2.70	37.08	Red

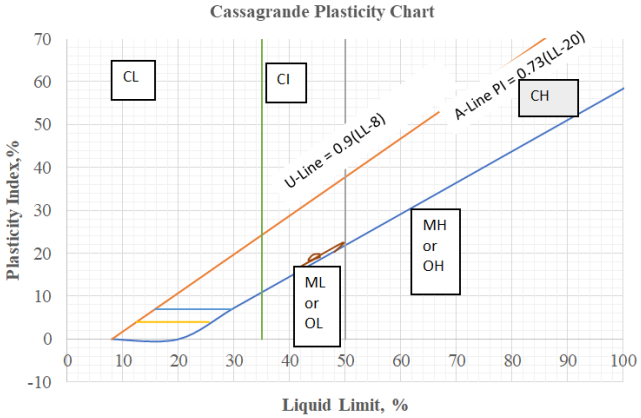


Figure 3. *Study area Soil classification based on Plasticity chart.*

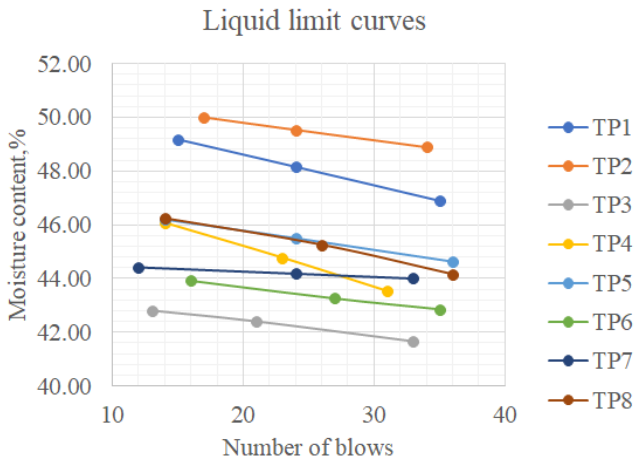


Figure 4. *Liquid limit curves.*

3.2. Compaction Characteristics

The compaction characteristics of Wolaita Sodo red clay were evaluated using the Modified Proctor procedure in accordance with ASTM D1557. The tests were performed to determine the Maximum Dry Density (MDD) and Optimum Moisture Content (OMC) of samples collected from TP1-TP8. The MDD values ranged from 1.52 g/cm^3 at TP2 to 1.66 g/cm^3 at TP7, with an average of approximately 1.58 g/cm^3. The corresponding OMC values ranged from 18.48% at TP7 to 28.12% at TP2, with an average of approximately 22.27%. The relatively high OMC values and moderate MDD values are consistent with the substantial fines content and water-retention capacity of the clay. Samples with higher clay contents require greater water contents to achieve adequate lubrication and particle rearrangement during compaction, but generally attain lower dry densities. These results highlight the importance of controlling both moisture content and field density during construction [17, 20]. For engineered fills, compaction should be carried out at or close to the laboratory-determined OMC and to the density specified in the applicable project requirements. The compaction parameters are summarized in Table 4, and the combined moisture-density curves are shown in Figure 5.

Table 4. *Compaction parameters of Wolaita Sodo red clay (ASTM D1557).*

Test pits	OMC (%)	MDD (g/cm^3)
TP1	26.25	1.53
TP2	28.12	1.52
TP3	21.81	1.57
TP4	20.5	1.6
TP5	24.30	1.54
TP6	20.14	1.58
TP7	18.48	1.66
TP8	18.53	1.63

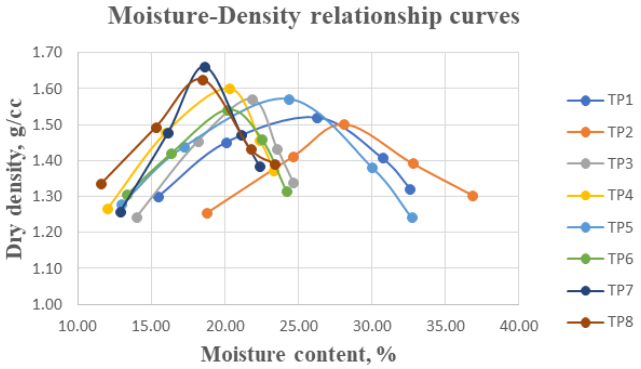


Figure 5. *Combined moisture-density relationship curves.*

3.3. Rate-Dependent Behavior in Unconsolidated Undrained Triaxial Tests

The effect of loading rate on total-stress undrained behavior was investigated using Unconsolidated Undrained (UU) triaxial compression tests on undisturbed specimens from TP1-TP4. The tests were conducted at axial displacement rates of 0.01, 0.1, and 1.0 mm/min under different confining pressures. The measured peak deviator stress, undrained shear strength, and axial strain at failure are summarized in Table 5.

Table 5. Summary of Unconsolidated Undrained (UU) triaxial test parameters under varying displacement rates.

Sample pit	Axial displacement rates (mm/min)	Confining pressure (kPa)	Peak deviator stress (kPa)	Undrained shear strength (kPa)	Axial strain at failure (%)
	0.01	50	123	61.5	16.02
	0.1	50	174.8	87.4	12.5
	1.0	50	226.6	113.3	9.5
	0.01	150	118.2	59.1	26
TP1	0.1	150	170.2	85	24.84
	1.0	150	221.8	110.9	18
	0.01	200	97.4	48.7	29
	0.1	200	170	74.6	26.5
	1.0	200	201	100.5	24.94
	0.01	80	281	140	13.12
	0.1	80	323.2	161.6	11.5
	1.0	80	365.3	182.6	10
	0.01	160	198.1	99.1	26.5
TP2	0.1	160	233	116	24.71
	1.0	160	267.95	133.98	23
	0.01	200	352.1	176	25.5
	0.1	200	427.6	251	23.5
	1.0	200	503	251	21.23
	0.01	40	249	125	25.5
	0.1	40	286.4	143.2	21.5
	1.0	40	311.3	155.6	18.5
	0.01	80	211.7	105.8	27.5
TP3	0.1	80	249	125	25.05
	1.0	80	298.8	149.4	20.5
	0.01	120	368.2	184.1	29
	0.1	120	415.4	207.7	27
	1.0	120	472	236	25.02
	0.01	45	332	166	25.13
	0.1	45	382.8	190.9	23.6
	1.0	45	431.6	215.8	22.1
	0.01	100	352	176	25.1
TP4	0.1	100	391	200.9	22.43
	1.0	100	441.6	225.8	21.13
	0.01	150	400	200	21.5
	0.1	150	465	232.5	19.5
	1.0	150	548	274	17.92

3.3.1. Effect of Loading Rate on Peak Deviator Stress and Undrained Shear Strength

The UU test results generally demonstrate pronounced rate-dependent behavior. For most test conditions, increasing the axial displacement rate from 0.01 to 1.0 mm/min increased both Peak deviator stress and Undrained shear strength. For example, for TP1 at a confining pressure of 50 kPa, Peak deviator stress increased from 123.0 kPa at 0.01 mm/min to 174.8 kPa at 0.1 mm/min and 226.6 kPa at 1.0 mm/min. The corresponding undrained shear strength increased from 61.5 to 87.4 and 113.3 kPa, respectively. Relative to the lowest rate, the peak deviator stress increased by approximately 42.1% at 0.1 mm/min and 84.2% at 1.0 mm/min. This increase may be attributed to viscous resistance, restricted creep, and insufficient time for particle rearrangement and pore-pressure redistribution during rapid shearing [6, 21].

3.3.2. Effect of Loading Rate on Failure Strain

The axial strain at failure generally decreased as the displacement rate increased. For example, in TP1 at a confining pressure of 50 kPa, axial strain at failure decreased from 16.02% at 0.01 mm/min to 12.50% at 0.1 mm/min and 9.50% at 1.0 mm/min. This trend suggests a transition from relatively ductile behavior at low loading rates to more brittle behavior at high rates. Under slow shearing, creep and progressive particle rearrangement allow greater deformation before peak strength is reached. In contrast, rapid loading limits structural relaxation and promotes earlier localization of deformation and shear failure [22, 23].

3.4. Rate-Dependent Behavior in Consolidated Undrained Triaxial Tests

Consolidated Undrained (CU) triaxial tests with pore-water-pressure measurement were conducted to evaluate the effective-stress response of the red clay. The effective confining pressure ($\sigma_{3'}$), major effective principal stress at failure ($\sigma_{1'}$), peak deviator stress, effective cohesion (c'), and effective friction angle (ϕ') are summarized in Table 6.

Table 6. *Summary of Consolidated Undrained (CU) triaxial test parameters under varying displacement rates.*

Sample pit	Strain rate (mm/min)	Effective Confining pressure (kPa)	Major effective principal stress (kPa)	Peak deviator stress (kPa)	Effective cohesion, c' (kPa)	Effective friction angle, ϕ' (°)
	0.01	78.6	318.9	240.3	42.9	24
	0.1	78.6	342.9	264.3	44	26
	1.0	78.6	367	288.4	44.8	28
	0.01	158.1	555	396.9	44.59	25
TP1	0.1	158.1	575.5	417.4	44.65	26
	1.0	158.1	596	437.9	45.61	28
	0.01	196.3	520.3	324	50.1	23.03
	0.1	196.3	539.8	343.5	63.27	24.38
	1.0	196.3	559.3	363	64.62	25.67
	0.01	85.6	348.5	262.9	35.2	23.6
	0.1	85.6	367.7	282.1	41.4	25.4
	1.0	85.6	387.7	302.1	48.2	27.2
	0.01	170	522.4	340	35.51	23.1
TP2	0.1	170	542.4	360	42.76	24.3
	1.0	170	562.4	380	49.81	25
	0.01	255	670	415	40.1	23.03
	0.1	255	685	430	53.27	24.38
	1.0	255	715	460	56.62	25.67
TP3	0.01	45.9	301.5	255.6	55	20

Sample pit	Strain rate (mm/min)	Effective Confining pressure (kPa)	Major effective principal stress (kPa)	Peak deviator stress (kPa)	Effective cohesion, c' (kPa)	Effective friction angle, ϕ' (°)
	0.1	45.9	342.9	268.3	60	24
	1.0	45.9	367	288.4	70	27
	0.01	89.1	264.6	178.5	55	20
	0.1	89.1	265.3	191	60	24
	1.0	89.1	292.7	203.6	70	27
	0.01	118.4	336.2	217.8	51.15	25.5
	0.1	118.4	352.4	234	59.25	26
	1.0	118.4	363.9	250.3	67.4	28
	0.01	76.7	447.6	370.9	41.9	22.3
	0.1	76.7	468.2	392	44.5	24.2
	1.0	76.7	491.7	415	45	25
	0.01	154	678.5	524.5	43.9	25
TP4	0.1	154	689	535	44.6	26
	1.0	154	706	552	45.8	28.6
	0.01	230	872	534	42.1	21.3
	0.1	230	1000.4	560	46.8	23.2
	1.0	230	1129	575	50.3	24.2

The CU results generally show that increasing the axial displacement rate increased the peak deviator stress. For example, for TP1 at $\sigma_{3'}$=78.6 kPa, Peak deviator stress increased from 240.3 kPa at 0.01 mm/min to 264.3 kPa at 0.1 mm/min and 288.4 kPa at 1.0 mm/min. Similar trends were observed for most of the tested specimens. The increase in strength with loading rate is consistent with the limited time available for pore-pressure redistribution and microstructural relaxation during rapid shearing.

3.5. Rate-Dependent Variation of Effective Strength Parameters

The effective strength parameters derived from the CU tests generally increased with increasing axial displacement rate, although the magnitude of the increase varied with test pit and confining pressure. For TP1 at $\sigma_{3'}$=78.6 kPa, (c') increased from 42.90 kPa at 0.01 mm/min to 44.80 kPa at 1.0 mm/min, while ϕ' increased from 24.0° to 28.0°. For TP2 at $\sigma_{3'}$=85.6 kPa, (c') increased from 35.20 to 48.20 kPa and ϕ' increased from 23.6 °to 27.2 °over the same rate range. These apparent increases may reflect enhanced viscous resistance, restricted pore-pressure dissipation, and reduced time for particle rearrangement during rapid shearing [1, 7, 14].

3.6. Comparison of CU and UU Strengths

The CU and UU results should be compared cautiously because the tests were conducted under different stress histories and, in some cases, different confining pressures. For example, TP1 produced a CU peak deviator stress of 240.3 kPa at an effective confining pressure of 78.6 kPa and a displacement rate of 0.01 mm/min, whereas the UU test produced 123.0 kPa at a total confining pressure of 50 kPa and the same nominal displacement rate. The higher CU strength is consistent with the preceding consolidation stage, which reduces the void ratio and changes the soil fabric before undrained shearing. Therefore, the difference cannot be attributed solely to the test type, it also reflects differences in consolidation history, effective stress, and confining pressure.

4. Conclusions

This study investigated the physical properties, compaction behavior, and rate-dependent shear response of tropical residual red clay from Wolaita Sodo City, Ethiopia. The soil contained a high fines fraction, ranging from 77.20% to 88.97%, and exhibited average values of 36.47% for natural moisture content, 2.65 for specific gravity, 45.31% for Liquid Limit, and 19.44% for Plasticity Index. The samples were classified

as inorganic clay of intermediate plasticity (CI) under the USCS and A-7-6 under the AASHTO system. Modified Proctor tests produced MDD values of 1.52-1.66 g/cm^3 and OMC values of 18.48-28.12%. The UU and CU triaxial tests demonstrated that increasing the axial displacement rate from 0.01 to 1.0 mm/min generally increased peak deviator stress and undrained shear strength, while reducing axial strain at failure. This behavior indicates increased apparent resistance and a transition from more ductile to more brittle deformation under rapid shearing. The CU tests also showed rate-dependent variations in the derived effective strength parameters, (c') and ϕ', although the magnitude of these changes varied with confining pressure and test location. The results confirm that loading-rate effects should be considered when selecting design parameters for foundations, excavations, embankments, and other infrastructure constructed on Wolaita Sodo red clay.

Abbreviations

UU	Unconsolidated Undrained Triaxial Test
CU	Consolidated Undrained Triaxial Test
c'	Effective Cohesion
ϕ'	Effective Friction Angle
σ'_3	Minor Effective Principal Stress
q_{max}	Peak Deviator Stress
MDD	Maximum Dry Density
OMC	Optimum Moisture Content
kPa	Kilo Pascal
CI	Intermediate Plasticity
DMS	Degree Minute Second
GPS	Global Positioning System

Author Contributions

Wopnesh Bassa Beyene: Conceptualization, Data curation, Formal Analysis, Investigation, Methodology, Writing – original draft

Eyob Shanka Koyra: Formal Analysis, Investigation, Writing – review & editing

Jemal Aliy Gobena: Supervision

Data Availability Statement

All data generated or analyzed during this study are included in this published article.

Conflicts of Interest

The authors declare no conflict of interest.

References

[1] H. Xu, Y. Zhao, W. Ding, and P. Cheng, "Experimental study on the influence of clay content on the shear strength of silty soil and mechanism analysis," Applied Sciences, vol. 14, no. 8, art. no. 3178, pp. 1-16, 2024, https://doi.org/10.3390/app14083178

[2] S. Mohammed, A. Kassahun, and A. Ahmed, "An inclusive study on the effect of strain rate on the stress-strain behavior and the undrained shear strength of clay soils in Kombolcha, Ethiopia," Engineering, Technology & Applied Science Research, vol. 12, no. 1, pp. 8107-8113, 2022, https://doi.org/10.48084/etasr.4626

[3] E. A. Ozsoy and H. B. Özmen, "Investigation of the shear strength behavior of clay soil reinforced with basalt fiber using ring shear tests," Buildings, vol. 16, no. 1, pp. 1-16, 2026, https://doi.org/10.3390/buildings16010045

[4] A. Tirualem, "Effect of strain rate on stress-strain relationship and shear strength of Addis Ababa red clay," M. Sc. thesis, Department of Civil Engineering, Addis Ababa University, Addis Ababa, Ethiopia, 2011.

[5] F. Cheng, X. Zhang, and Q. Li, "Interfacial shear properties of red clay and polyurethane with different densities," Polymers, vol. 17, no. 3, pp. 1-15, 2025, https://doi.org/10.3390/polym17030412

[6] P. Iqbal, R. F. Susanti, and A. Mulyana, "Geotechnical characteristics of volcanic red clay soil related to geoengineering problem in Sekincau, Sumatra, Indonesia," International Journal of Advanced Science and Technology, vol. 29, no. 7, pp. 3166-3173, 2020.

[7] Y. Chen, B. Li, Y. Xu, Y. Zhao, and J. Xu, "Field study on the soil water characteristics of shallow layers on red clay slopes and its application in stability analysis," Arabian Journal for Science and Engineering, vol. 44, no. 5, pp. 5107-5116, 2019, https://doi.org/10.1007/s13369-018-03716-3

[8] W. Chinkhuntha, A. Owayo, and N. Ambassah, "Performance evaluation of red clay soils stabilized with bluegum sawdust ash and sisal fiber as low-volume road sub-base materials," Engineering, Technology & Applied Science Research, vol. 14, no. 6, pp. 18105-18113, 2024, https://doi.org/10.48084/etasr.8772

[9] A. Tadese, E. Getahun, M. Jothimani, and T. Demisie, "Engineering geological characterization of soils and rocks for urban planning: A case study from Wolaita Sodo Town, Southern Ethiopia," Urban Science, vol. 9, no. 1, art. no. 124, pp. 1-39, 2025, https://doi.org/10.3390/urbansci9010124

[10] M. S. Senthil and E. S. M. Suresh, "Study on geotechnical, engineering and chemical analysis of amended red soil as landfill liner material," Sambodhi Journal, vol. 44, no. 2, pp. 212-220, 2021.

[11] T. B. Esubalew and W. Wondemagne, "Stabilization of expansive soil by using A-1-b soil in subgrade materials: A study in Boditi Town, Wolaita Zone, Southern Ethiopia," Journal of University of Shanghai for Science and Technology, vol. 24, no. 1, pp. 346-357, 2022, https://doi.org/10.51201/jusst/22/0146

[12] G. A. Gizachew, "Improving the geotechnical property of expansive soil through marble dust and lime for road construction projects," International Research Journal of Engineering and Technology, vol. 6, no. 10, pp. 1497-1504, 2019.

[13] J. A. Gobena and S. Suppiah, "Strength characteristics of expansive soil mixed with quarry residue and cement," International Journal of Innovative Technology and Exploring Engineering, vol. 8, no. 8, pp. 1668-1673, 2019.

[14] T. Hanna, "Study of index properties and shear strength parameters of laterite soils in southern part of Ethiopia: The case of Wolayita-Sodo," M. Sc. thesis, School of Graduate Studies, Addis Ababa University, Addis Ababa, Ethiopia, 2008.

[15] A. C. Yan, "Stabilization of clayey soil using lime and lime with Prosopis juliflora fibers in Jimma Town, Ethiopia," M. Sc. thesis, Faculty of Civil and Environmental Engineering, Jimma Institute of Technology, Jimma University, Jimma, Ethiopia, 2021.

[16] S. Zheng, D. Qi, X. Guo, X. Xi, and L. Zhang, "Characterization of the undrained shear strength of expansive soils of high water content," MATEC Web of Conferences, vol. 206, art. no. 01002, pp. 1-5, 2018, https://doi.org/10.1051/matecconf/201820601002

[17] A. Olowofoyeku, O. Ofuyatan, J. Oluwafemi, and P. Iroaganachi, "Geotechnical properties of lateritic soil stabilized with sugarcane straw ash," Journal of Physics: Conference Series, vol. 1734, no. 1, art. no. 012011, pp. 1-5, 2021, https://doi.org/10.1088/1742-6596/1734/1/012011

[18] E. A. Gaenamo, D. D. Dirate, D. K. Dasho, and V. R. Pampana, "Experimental investigation and mapping of index and shear behavior of soils: A case in Gimbichu Town, Ethiopia," Indian Journal of Science and Technology, vol. 15, no. 4, pp. 166-174, 2022, https://doi.org/10.17485/ijst/v15i4.1868

[19] S. A. Sule, S. I. Maude, U. Adamu, and M. A. Mailafiya, "Investigation of index properties of soils along Jos-Makurdi Road in North Central Nigeria," Saudi Journal of Civil Engineering, vol. 5, no. 4, pp. 87-90, 2021, https://doi.org/10.36348/sjce.2021.v05i04.002

[20] D. Gudissa, S. Thanappan, and E. Mekonnen, "The stabilization of lateritic soils: Trends in Africa/Ethiopia," Journal of Xidian University, vol. 14, no. 11, pp. 328-335, 2020, https://doi.org/10.37896/jxu14.11/030

[21] Q. Dai, X. Shen, C. Wei, and Z. Zhou, "Shear failure mechanism and shear zone morphology of red-bed soft rock at different strain rates," Applied Sciences, vol. 16, no. 2, pp. 1-17, 2026, https://doi.org/10.3390/app16020512

[22] Geotechnical Engineering Office, "The determination of shear strength in residual soils," Civil Engineering Department, The Government of the Hong Kong Special Administrative Region, GEO Report No. 110, pp. 1-18, 2001.

[23] F. Jamil, C. Zeng, Y. Ma, S. H. Tun, and S. Ali, "Shear stress-strain relationships and anisotropy in silty soil: The role of principal stress rotation," Acta Geodynamica et Geomaterialia, vol. 21, no. 4, pp. 309-328, 2024, https://doi.org/10.13168/AGG.2024.0026